Stability of the axial director configuration in nematic liquid crystals confined in a cylindrical cavity and the surface-like elastic constant problem

A. D. Kiselev

Chernigov Technological Institute, 250027 Chernigov, Ukraine

V. Yu. Reshetnyak

Surface Chemistry Institute of the Ukrainian Academy of Sciences, 252000 Kiev, Ukraine

(Submitted 12 October 1994)
Zh. Éksp. Teor. Fiz. **107**, 1552–1562 (May 1995)

Nematic liquid crystals confined in a cylindrical cavity under the anchoring conditions of various type are examined. The influence of the saddle—splay and splay—bend terms (the K_{24} term and the K_{13} term) on the axial director configuration stability is investigated. By using the Fourier expansion of director fluctuations over the azimuth angle our analytical method of attack enables the stability conditions to be found in terms of the stability of each fluctuation mode. Two methods of stabilizing the structure are explored: stabilization by a magnetic field and by the action of the boundary conditions. The restrictions imposed on the constants are determined to make the stabilization possible. The dependence of the resultant stability threshold on the surface-like elastic constants is calculated. The experimentally detectable effects due to the presence of the K_{13} term are discussed in detail. It is shown that the escaped—radial director structure exhibits some special features which are induced by the K_{13} term. © *1995 American Institute of Physics.*

1. INTRODUCTION

It was shown in Refs. 1–3 that, in addition to the usual Frank terms (splay plus twist plus bend), the nematic free energy contains so-called surface-like elastic terms, i.e., two terms of the divergence form, which can be transformed into integrals over the boundary surface and which are proportional to the saddle-splay elastic constant, K_{24}, and the splay-bend constant, K_{13}. They can be written in the form:

$$F_{24}=-\frac{K_{24}}{2}\int_{v} dv\ \mathrm{div}[\mathbf{n}\ \mathrm{div}\ \mathbf{n}+[\mathbf{n}\ \mathrm{curl}\ \mathbf{n}]], \tag{1}$$

$$F_{13}=\frac{K_{13}}{2}\int_{v} dv\ \mathrm{div}[\mathbf{n}\ \mathrm{div}\ \mathbf{n}], \tag{2}$$

where $\mathbf{n}$ is the nematic director field.

The surface terms are irrelevant if we are interested in the bulk properties of NLC, but they are of considerable importance in the understanding of the physical properties of NLC confined in geometries more restrictive than bulk geometries. Two points must be considered dealing with the surface elastic constant problem: Is it possible for the surface-like elastic terms to be taken into account in the framework of the liquid-crystal continuum theory unambiguously? What are the effects caused by the presence of the K_{24} and K_{13} terms?

Taking up first the K_{24}-problem, the case when the K_{13}-term is disregarded, it is safe to say that the answer to the first question is affirmative and the problem of minimizing the free energy with the K_{24} term was shown to be always well posed, because this term does not contain the director derivatives along the directions normal to the boundary surface.[4,5] Hence the K_{24} term affects only the standard boundary conditions. The second question has recently been given considerable attention. Physical effects whose very occurrence critically depends on the value of K_{24} have been shown to exist,[5–7] and even estimates of the value of K_{24} have been given.[8,9]

In contrast with the K_{24} problem, the issue concerning the K_{13} term is much more questionable. In the strict sense, the free energy functional with the K_{13} term has no lower bound, which accounts for the strong spontaneous substrate director deformations.[10] One way to avoid such an unphysical effect, which was proposed in Refs. 11 and 12, is to search for the director distribution which minimizes the free energy functional among the solutions to the Euler–Lagrange equations. We will not discuss other ways of looking at the problem[13,14] and will use the approach discussed above to study how the surface-like terms affect the stability threshold of the axial director configuration for NLC confined to a cylindrical cavity in the presence of a stabilizing magnetic field under various anchoring conditions.

In Sec. 2, we analyze the stability in the one-constant approximation. Using the Fourier expansion of the director fluctuation over the azimuth angle, we derive unequalities which give the stability condition for the axial structure of each fluctuation harmonic. We explore two ways of stabilizing the structure in question: stabilization by the magnetic field and stabilization by the action of boundary conditions. In each case we imposed restrictions on the values of K_{13} and K_{24} under the assumption that the configuration can be stabilized. The stabilization appears to be possible provided that the quantity $K_{13}/4K$ takes the values lying between $q_{24}-(q_{24})^{1/2}$ and $q_{24}+(q_{24})^{1/2}$, where the notation q_{24} denotes $K_{24}/2K$. We also discuss whether the fluctuation mode, which defines the resultant stability threshold, can be changed by the magnetic field or by the anchoring energy at

 1063-7761/95/050867-06$10.00

the given values of K_{24} and K_{13}. The results of numerical calculations are presented.

The escaped-radial director configuration is investigated in Sec. 3. The stability threshold to zero-numbered fluctuation mode is shown to describe the transition between the axial structure and the escaped-radial structure. A comparison of the energies shows that there are the values of K_{13} at which the stability condition does not provide the global stability of the axial pattern. The K_{13} term which was found may produce an additional degree of energy degeneracy, which in turn would result in the appearance of a disclination circle at the surface.

Some additional comments on the K_{13} problem are made in Sec. 4.

2. STABILITY OF AXIAL DIRECTOR CONFIGURATION

Let us consider a nematic liquid crystal which is confined to the cylindrical cavity of radius R in the presence of a magnetic field applied along the cavity axis, $\mathbf{H}=H\mathbf{e}_z$. The nematic liquid crystal free energy may be taken in the standard form

$$F=\frac{K}{2}\int_v dv[(\text{div }\mathbf{n})^2+(\text{curl }\mathbf{n})^2-q^2n_z^2]+F_{24}+F_{13}-\frac{W_h}{2}\int_s ds(\mathbf{n}\mathbf{e}_R)^2-\frac{W_p}{2}\int_s ds(\mathbf{n}\mathbf{e}_z)^2. \tag{3}$$

Here we use an one-constant approximation, and $q^2=\chi_a H^2/K$ (q^{-1} is the magnetic coherent length, and χ_a is the anisotropic part of the magnetic susceptibility, which is assumed to be positive). In Eq. (3) the energy of the interaction between the nematic liquid crystal and the cavity wall is given as a sum of two addends written in the Rapini–Papoular form.[15] The first term is the anchoring energy under the homeotropic boundary conditions (the vector of easy orientation is normal to the confining surface) and the last term represents the anchoring energy under the planar boundary conditions (the vector of easy orientation is directed along the cavity axis). Beginning with the stability analysis, it is convenient to write the director in the cylindrical coordinate system (the z axis is parallel to the cavity axis) as follows:

$$\mathbf{n}=\cos\Theta\cos\Phi\mathbf{e}_z+\cos\Theta\sin\Phi\mathbf{e}_R+\sin\Theta\mathbf{e}_\varphi, \tag{4}$$

where $\Theta=\Theta(r,\varphi)$, and $\Phi=\Phi(r,\varphi)$. Evidently, the axial director distribution ($\mathbf{n}_0=\mathbf{e}_z$) can be determined from Eq. (4) by setting $\Theta=\Phi=0$. Below we shall use the notation θ and ϕ for small deviations of the angles Θ and Φ from zero.

To study the axial configuration stability, we must substitute the director field given by Eq. (4) into the expression for the nematic liquid crystal free energy [Eq. (3)] and derive the second-order variation of the free energy functional as a bilinear part of the energy in the angle fluctuations θ and ϕ. We can write the result in the form

$$\delta^2F=\frac{K}{2}\int_0^{2\pi}d\varphi\int_0^R rdr\left\{\left[\frac{\phi}{r}+\frac{\partial\phi}{\partial r}+\frac{1}{r}\frac{\partial\theta}{\partial\varphi}\right]^2+\left[\frac{\theta}{r}+\frac{\partial\theta}{\partial r}-\frac{1}{r}\frac{\partial\phi}{\partial\varphi}\right]^2\right\}+\delta^2F_{24}+\delta^2F_{13}+\delta^2F_s, \tag{5}$$

where

$$\delta^2F_{24}=-\frac{K_{24}}{2}\int_0^{2\pi}d\varphi\left[\phi^2+\theta^2+\phi\frac{\partial\theta}{\partial\varphi}-\theta\frac{\partial\phi}{\partial\varphi}\right]_{r=R}, \tag{6}$$

$$\delta^2F_{13}=\frac{K_{13}}{2}\int_0^{2\pi}d\varphi\left[\phi^2+\phi\frac{\partial\theta}{\partial\varphi}+R\phi\frac{\partial\phi}{\partial r}\right]_{r=R}, \tag{7}$$

$$\delta^2F_s=-\frac{R}{2}\int_0^{2\pi}d\varphi[W_h\phi^2-W_p(\phi^2+\theta^2)]_{r=R}. \tag{8}$$

The Euler–Lagrange equations for the functional δ^2F are given by

$$\begin{bmatrix}\Delta-1-q^2r^2 & 2\dfrac{\partial}{\partial\varphi}\\ -2\dfrac{\partial}{\partial\varphi} & \Delta-1-q^2r^2\end{bmatrix}\begin{bmatrix}\theta\\ \phi\end{bmatrix}=0, \tag{9}$$

where

$$\Delta=\left(r\frac{\partial}{\partial r}\right)^2+\left(\frac{\partial}{\partial\varphi}\right)^2.$$

Since the angle fluctuations are 2π-periodic functions of the azimuth angle, they can be expanded in the Fourier series over φ.

$$\theta=(2\pi)^{-1/2}\sum_{m=-\infty}^{\infty}\theta_m(r)\exp(im\varphi), \tag{10a}$$

$$\phi=(2\pi)^{-1/2}\sum_{m=-\infty}^{\infty}\phi_m(r)\exp(im\varphi). \tag{10b}$$

To solve the Euler–Lagrange equations we introduce the new Fourier amplitudes in the following way:

$$\phi_m^1(r)=(\phi_m(r)+i\theta_m(r))/2, \tag{11a}$$

$$\theta_m^1(r)=(\phi_m(r)-i\theta_m(r))/2. \tag{11b}$$

Using Eqs. (9)–(11), we can easily find the equations for these fluctuation harmonics amplitudes:

$$\Delta_{m+1}\phi_m^1=0,\quad \Delta_{m-1}\theta_m^1=0, \tag{12}$$

where

$$\Delta_{m\pm1}=\left(r\frac{\partial}{\partial r}\right)^2-(m\pm1)^2-q^2r^2.$$

The solutions to the equations (12) are expressed in terms of modified Bessel functions:[16]

$$\theta_m^1(r)=C_m^1I_{|m-1|}(qr),\quad \phi_m^1(r)=C_m^2I_{m+1}(qr), \tag{13}$$

where C_m^j are the complex coefficients ($\text{Re }C_m^j=A_m^j$, $\text{Im }C_m^j=B_m^j$, and $j=1,2$), $I_m(x)$ is the modified Bessel function of order m.

Inserting Eqs. (10), (11), and (13) into Eq. (5) and performing rather routine calculations, we obtain

$$\delta^2 F=\sum_{m=0}^{\infty}[\delta^2 F_m(A)+\delta^2 F_m(B)], \tag{14}$$

$$\begin{aligned}\delta^2 F_m(A)=&(A_m^1)^2\{(K+K_{13}/2)xI_{|m-1|}(x)I_m(x)\\&+I_{|m-1|}^2(x)(K_{24}(m-1)-WR/2)\}\\&+(A_m^2)^2\{(K+K_{13}/2)xI_{m+1}(x)I_m(x)\\&-I_{m+1}^2(x)(K_{24}(m+1)+WR/2)\}\\&+A_m^1A_m^2\{K_{13}xI_m(x)(I_{m+1}(x)+I_{|m-1|}(x))/2\\&-I_{m+1}(x)I_{|m-1|}(x)W_hR\},\end{aligned} \tag{15}$$

where $x=qR$, and $W=W_h-2W_p$.

For the axial configuration to be stable, all the quadratic forms $\delta^2F_m(A)$ should be positive definite, so that the condition of the axial structure stability is given by a set of inequalities which describe the stability to each fluctuation harmonic specified by the number m. Standard algebraic analysis shows that the stability conditions for δ^2F_m can be taken in the form suitable for subsequent discussion:

$$m=0:\quad \begin{cases} w_h<(1+2q_{13})\gamma_{+1}(x)-q_{24}+w_p=T_0(x),\\ 0<\gamma_{+1}(x)-q_{24}+w_p=p_0(x),\end{cases} \tag{16a}$$

$$m>0:\quad \begin{cases} w_h<T_m(x)=t_m(x)/2p_m(x),\\ 0<p_m(x)=\alpha_m(x)+\beta_m(x)-2q_{24}+2w_p,\end{cases} \tag{16b}$$

where

$$\gamma_{m+1}(x)=\frac{xI_m(x)}{2(m+1)I_{m+1}(x)}=\frac{\beta_m(x)}{m+1}, \tag{17a}$$

$$\gamma_{m-1}(x)=\frac{2mI_m(x)}{xI_{m-1}(x)}=4m\alpha_m(x)x^{-2}, \tag{17b}$$

$$\begin{aligned}t_m(x)=&-q_{13}^2(\alpha_m(x)-\beta_m(x))^2+4q_{13}(\alpha_m(x)[2\beta_m(x)\\&-(m+1)q_{24}]+q_{24}(m-1)\beta_m(x)+w_p(\alpha_m(x)\\&+\beta_m(x)))+4(\alpha_m(x)+(m-1)q_{24}+w_p)\\&\times(\beta_m(x)-(m+1)q_{24}+w_p).\end{aligned} \tag{18}$$

We used the following notation for the four dimensionless parameters: $w_h=W_hR/2K$, $w_p=W_pR/2K$, $q_{24}=K_{24}/2K$, and $q_{13}=K_{13}/2K$.

Since the parameter w_h is nonnegative, we can define the resultant stability threshold as the greatest lower bound of the quantities, which govern the stability of each fluctuation mode:

$$W_c(x)=\inf_m\{TR_m(x)\}, \tag{19}$$

$$TR_m(x)=\begin{cases}T_m(x), & \text{if } T_m(x)>0 \text{ and } p_m(x)>0,\\ 0, & \text{otherwise.}\end{cases} \tag{20}$$

Then the stability condition becomes

$$w_h<W_c(x). \tag{21}$$

Let us consider the notation used above. It is clear that all the functions in Eqs. (16)–(21), except $\gamma_m(x)$, $\alpha_m(x)$, and $\beta_m(x)$, depend on the dimensionless parameters w_p, q_{24} and q_{13}, which were omitted in the notation for brevity.

In what follows we consider whether it is possible for the axial director pattern to be stabilized either by applying the magnetic field or by increasing the anchoring energy W_p. Mathematically, the magnetic field fails to stabilize the axial configuration under the homeotropic anchoring conditions if $W_c(x)=0$ at $w_p=0$ for all $x>0$. In the other case of $W_c(0)=0$ for all $w_p>0$ we find the configuration to be unstable, even though the boundary conditions make the molecules of the NLC orient along the cavity axis.

2.1. Influence of the K_{24} term on the stability threshold

In this subsection we consider the case of $K_{13}=0$. First, it is useful to point out several simple properties of the functions $\gamma_{m\pm1}(x)$:

a) $\gamma_{m\pm1}(0)=1$;

b) $\gamma_{m+1}(x)>1$, $\gamma_{m-1}(x)<1$ for nonzero values of x;

c) $\gamma_{m\pm1}(x)$ monotonically tend to unity as m goes to infinity.

There is no need to make numerical calculation to conclude that the axial structure cannot be stabilized by the magnetic field if the value of q_{24} does not lie within the interval (0,1). In other words, it means that for a given value of x there is a number m such that either $p_m(x)<0$ or $T_m(x)<0$ if q_{24} takes the value which is outside the interval (0,1). To prove our contention, let q_{24} initially be negative, so that $p_m(x)>0$ for any m. The expression for $t_m(x)$ can be derived from Eq. (18) by setting $w_p=q_{13}=0$.

$$t_m(x)=4(m+1)[\alpha_m+(m-1)q_{24}][\gamma_{m+1}-q_{24}]. \tag{22}$$

Clearly, the sign of $t_m(x)$ is dictated by the first factor enclosed in square brackets. It is yet to be determined whether the factor goes negative if m is a sufficiently large number, since $\alpha_m(x)$ goes to zero as $m\to\infty$ [see Eq. (17b)]. If q_{24} is greater than unity, it is sufficient to note that $\gamma_{m+1}(x)$ is a monotonically decreasing function of m, which tends to unity as $m\to\infty$, and therefore the second factor in Eq. (22), which is enclosed in square brackets, goes negative, beginning with a sufficiently large number m, whereas the first factor is positive.

In the case of stabilization by the action of the boundary conditions ($x=0$ and $w_p>0$) we easily come to a similar conclusion. Since $\alpha_m(0)=0$ and $\beta_m(0)=m+1$, we obtain from Eq. (18) the expression

$$\begin{aligned}t_m(0)=&4(m+1)[w_p+(m-1)q_{24}]\\&\times[1-q_{24}+w_p/(m+1)].\end{aligned} \tag{23}$$

It is clear that $t_m(0)$ goes negative at a sufficiently large number m, when q_{24} is outside the interval [0,1].

The same restrictions on q_{24} were found to hold in the case of a spherical geometry.[17] These restrictions are more rigid than those given by Ericksen.[18] The latter can be rewritten in our denotion as follows: $0<q_{24}<2$. Note that the values of q_{24} extracted from the deuterium nuclear-magnetic-resonance experiments on submicrometer-size, nematic, cylindrical cavities typically fall in the range 0.5–0.8 for

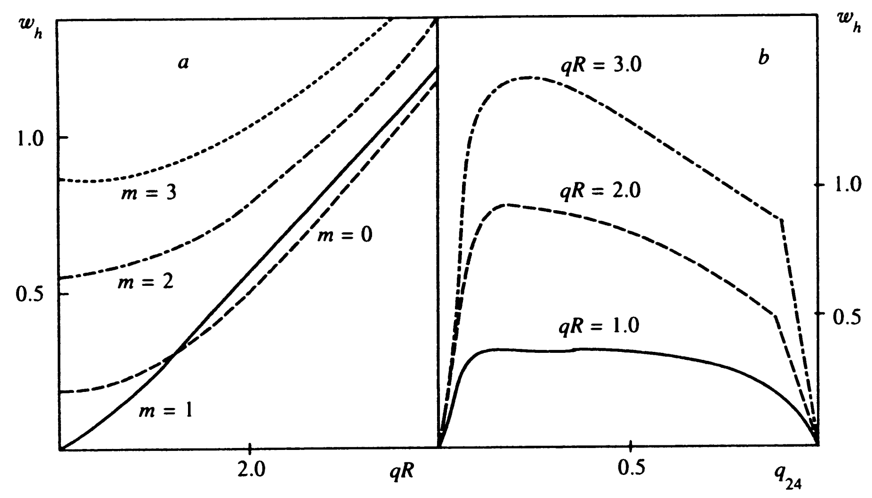

FIG. 1. (a) The plots of TR_m versus qR in the w_h-qR plane for $m=0-3$ at $q_{24}=0.8$. The stability region is located below the lowest curves. (b) The stability diagram in the w_h-q_{24} plane at $qR=1-3$. For a given value of qR the area of the stability is enclosed by the curve and the q_{24} axis.

$5CB-\beta d_2$ with $K=5\cdot 10^{-12}$ J/m, $W_p=3\cdot 10^{-5}$ J/m^2, and $q^{-1}=1.7$ μm ($H=4.7$ T).[9,19] Clearly, the axial structure is unstable under the specified conditions. To have a stable structure one has to greatly reduce the anchoring energy W_p or to increase the magnetic field. For example, W_p should be on the order of $5\cdot 10^{-7}$ J/m^2 for a cavity radius $R=q^{-1}=1.7$ μm.

The plots of TR_m in relation to $x=qR$, shown in Fig. 1a for $q_{24}=0.8$ and $m=0-3$, illustrate how the curves TR_m form the threshold line W_c in the $w-qR$ plane. We see that the first fluctuation mode ($m=1$) defines the stability threshold in the case of small magnetic field strength $[TR_1(0)=0]$, but the number of the mode, which governs the threshold, changes to zero as the field strength increases. The modes, which contribute to the resultant stability threshold at various x, increases in number as the quantity q_{24} approaches zero or unity. Interestingly, $TR_m(x)$ are not equal to zero for all m, if q_{24} takes a critical value (0 or 1) and $x\neq 0$, but $\lim TR_m=0$ as $m\to\infty$. As a result, $W_c(x)=0$ for all $x>0$. Hence, high-order harmonics play an important part in the vicinity of critical values of K_{24}, which causes the axial structure to be destabilized. The effect of destabilization is shown in Fig. 1b, where the plots of W_c as a function of q_{24} are shown for $qR=1,2,3$.

When the anchoring energy W_p is altered in order to gain the stabilization of the axial director structure, the situation which we encounter is quite different. Simple analysis shows that the fluctuation mode with $m=1$ alone determines the stability threshold $W_c(0)$:

$$W_c(0)=\frac{w_p(2-2q_{24}+w_p)}{1-q_{24}+w_p}. \tag{24}$$

It is therefore impossible to change the number of the fluctuation mode which contributes to the threshold. Nothing therefore prevents q_{24} now from being equal to zero or unity, and $W_c(0)$ is positive for all $w_p>0$.

2.2. Influence of the K_{13}-term on the stability threshold

Here we find out how the surface elastic constant K_{13} affects the axial pattern stability. We see from Eqs. (17a) and (17b) that the quantities $p_m(x)$ do not depend on K_{13}. Even if $q_{24}>1$, the condition $p_m(x)>0$ can be satisfied by choosing either an appropriate value of the field strength or the anchoring energy, W_p. Thus one has to analyze the expression for $t_m(x)$ as it was done above. Let us first consider the case of $x=0$ and $w_p>0$. From Eq. (18) we obtain:

$$t_m(0)=Am^2+2Bm+C, \tag{25}$$

where

$$A=-q_{13}^2+4q_{13}q_{24}+4q_{24}(1-q_{24}), \tag{26a}$$

$$B=-q_{13}^2+2q_{13}w_p+2w_p, \tag{26b}$$

$$C=-q_{13}^2+4q_{13}(w_p-q_{24})+4(w_p-q_{24})\times(w_p-q_{24}+1). \tag{26c}$$

The requirement $A>0$ places some restrictions on the values of q_{13} and q_{24}:

$$2[q_{24}-(q_{24})^{1/2}]<q_{13}<2[q_{24}+(q_{24})^{1/2}],\quad q_{24}>0, \tag{27a}$$

or

$$1+q_{13}-[1+2q_{13}]^{1/2}<2q_{24}<1+q_{13}+[1+2q_{13}]^{1/2},\quad q_{13}>-1/2. \tag{27b}$$

From the inequality $p_1(0)>0$ we have the threshold for w_p:

$$w_p>q_{24}-q_{13}-1+[(q_{24}-q_{13}-1)^2+q_{13}^2]^{1/2}. \tag{28}$$

The experimentally obtained estimate of K_{13} gives $q_{13}=-0.2$ for submicron nematic films[20] and we can obtain a rough estimate for the threshold $w_p>0.33$ at $q_{24}=0.7$, which implies $W_p>2\cdot 10^{-6}$ J/m^2 for $R=1.7$ μm and $K=5\cdot 10^{-12}$ J/m.

Using Eqs. (27) and (28), we can prove that the function $TR_m(0)$ is an increasing function of m for $m\geqslant 1$, and therefore $W_c=TR_1(0)$:

$$W_c=\frac{-q_{13}^2+w_p(w_p+2+2q_{13}-2q_{24})}{1+w_p-q_{24}}. \tag{29}$$

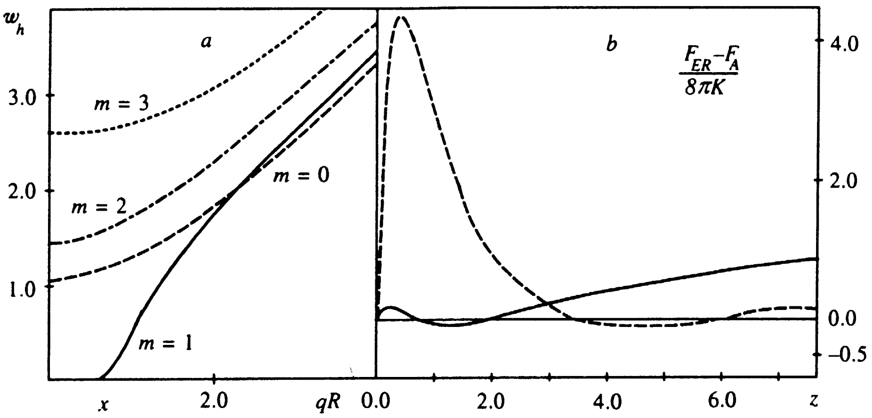

FIG. 2. (a) The qR dependence of TR_m in the w_h-qR plane for $q_{24}=0.8$ and $q_{13}=0.5$. The axial structure is shown to be unstable at $qR<x_c$. (b) The difference in energy of the escaped-radial configuration and the axial configuration, plotted as a function of the parameter z at $q_{24}=2.0$, $q_{13}=1.2$, $w_h=0.75$, and $w_p=0$ (solid line); $q_{24}=5.9$, $q_{13}=7.0$, $w_h=0.0$, and $w_p=0.05$ (dashed line).

Setting $q_{13}=0$, we have the result of the previous subsection: $0<q_{24}<1$ is a direct consequence of Eq. (27). In the same way, Eq. (28) gives $w_p>0$. The latter implies no threshold for w_p at $q_{13}=0$.

Looking again at the stabilization by the action of the magnetic field under the homeotropic anchoring conditions, $w_p=0$, we see that the restriction given by Eq. (27) remains in force, since the coefficient A of the quadratic polynomial in m in Eq. (25) differs from one in the case of nonzero magnetic field by quantities which tend to zero as $m\to\infty$. Interestingly, there are no restrictions on the upper limit of q_{24} which must be positive. We see in Fig. 2a that, even if $w_h=0$, the axial pattern is unstable until the strength of the magnetic field reaches its critical value, $x=x_c$, which strongly depends on q_{24} and q_{13}. From Eq. (23) we find that $t_1(0)<0$ at $w_p=0$. Therefore, it is necessary to apply a magnetic field of finite amplitude to make $t_1(0)$ positive. In the presence of the K_{13}-term both the magnetic field ($w_h\geqslant 0$, $w_p=0$) and the anchoring energy $W_p(x=w_h=0)$ must therefore exceed their threshold values to make the axial structure stable. Here we have the effects which can be detected experimentally. Both effects can be attributed to the appearance of a so-called spontaneously deformed state which arises as a result of the K_{13}-term. The latter was found to be realized in a planar nematic cell provided that $W_pd<4K_{13}-2K_{33}$ (d is the cell thickness).[21] Note that, contrastingly, we have the threshold for W_p in all cases of nonzero K_{13}.

In closing this subsection, it is pertinent to note that, in contrast with the stabilization by the action of the boundary conditions, we found that the magnetic field can change the fluctuation mode which governs the stability, so that the statement holds in the presence of the K_{13} term.

3. THE ESCAPED-RADIAL STRUCTURE IN THE PRESENCE OF THE K_{13} TERM

In what has been considered above, the K_{13} term is found to change the situation, both quantitatively and qualitatively. To clarify the role of the term, let us consider how the surface-like elastic constants affect the escaped-radial director structure.[22] The configuration was examined in Refs. 9 and 23 with the K_{24} term alone, but some new effects appear to be induced by the K_{13} term. The director field and the free energy for the structure under investigation are given by

$$\mathbf{n}=\sin\chi(r)\mathbf{e}_z+\cos\chi(r)\mathbf{e}_R, \tag{30}$$

$$\frac{F_{ER}}{\pi K}=\int_0^R\frac{dr}{r}\left[\cos^2\chi+\left(r\frac{d\chi}{dr}\right)^2\right]+\left[(1+2q_{13}-2q_{24}+2w_p-2w_h)\cos^2\chi-q_{13}\sin(2\chi)R\frac{d\chi}{dr}\right]_{r=R}-2w_p. \tag{31}$$

The solution of the Euler–Lagrange equation is

$$\sin\chi(r)=\frac{\rho^2-r^2}{\rho^2+r^2}, \tag{32}$$

where ρ is the integration constant. After substitution of Eq. (32) into Eq. (31) the free energy becomes

$$\frac{F_{ER}(z)}{(2\pi K)}=2z(1+z)^{-3}[z^2+(3-2q_{24}+2w_p-2w_h)z+2(1-q_{24}+w_p-w_h+2q_{13})]-w_p, \tag{33}$$

where $z=(R/\rho)^2$. It is easy to see that Eqs. (32) and (33) lead us to the axial structure, provided that $z=0$ and $F_A=2\pi Kw_p$. Therefore, the stability of the structure is governed by the sign of the term in the square brackets in Eq. (33). We see that the axial configuration is favorable in energy over the escaped-radial one when the term is positive for all $z>0$. Interestingly, the stability condition $w_h<T_0(0)$ yields an increase of $F_{ER}(z)$ at $z=0$, which means that the axial configuration is locally stable. If $K_{13}=0$, this condition is sufficient, but as evident from Fig. 2b, in the presence of the K_{13} term the local stability does not imply the global stability. In effect, one can obtain that the bracketed quadratic polynomial has two positive roots if

$$q_{24}-2q_{13}-2<w_p-w_h<q_{24}-2(q_{13})^{1/2}-0.5,\quad q_{13}>0.25. \tag{34}$$

Taking into account the restrictions given by Eq. (27), it is easy to conclude that inequalities Eq. (34) can be satisfied under the planar anchoring conditions ($w_h=0$) when q_{13} exceeds its critical value $q_{13}^c=6.41$ (see Fig. 2b). Thus we encounter here the effect which looks like a bistability caused by the K_{13} term and which is an explicit example of axial structure instability under the planar anchoring to the confining wall. For definiteness, we must point out the fact that Eq. (28) supplies a more rigid requirement for the axial configuration to be stable than the above-stated one, and it makes the difference $F_{ER}-F_A$ positive under the planar anchoring conditions, so that there is nothing to contradict our stability analysis and the effect may be attributed to the existence of the threshold for w_p.

Another effect which must be considered is connected with the escaped-radial configuration degeneracy in energy. The structure is known to be doubly degenerate due to the mirror symmetry $\chi\rightarrow-\chi$, which accounts for the appearance of the point defects along the cavity axis.[9] The K_{13} term may cause an increase in the degree of degeneracy in the event that the energy $F_{ER}(z)$ reaches a minimum at $z=z_{\min}>1$ (see Fig. 2b). If so, the new configuration of the same energy can be defined in the following way:

$$\sin\chi_-(r)=\begin{cases}\sin\chi(r), & r<\rho_{\min},\\ -\sin\chi(r), & \rho_{\min}\leqslant r\leqslant R,\end{cases}\tag{35}$$

where $\sin\chi(r)$ is given by Eq. (32) with $\rho=\rho_{\min}=R/\sqrt{z_{\min}}$. In the same manner as it had been shown for the mirror symmetry one can expect such kind of the degeneracy to produce circles of the disclinations at the surface. It must be emphasized that the K_{13} term need not necessarily have a value of $z_{\min}$ greater than unity, but $z_{\min}$ must always be less than unity if the term is ignored.

4. CONCLUSIONS

The stability analysis presented in this paper provides an insight into the surface-like elastic constant problem. In particular, the K_{24} term is shown to be of great importance for the axial configuration stability and must be taken into account to assure the stability. In contrast, we have found that the K_{13} term induces additional distortions, which result in the appearance of a threshold for the anchoring energy under the planar boundary conditions (no external fields) as well as for the magnetic field provided the surface is untreated (no anchoring). These effects can be tested experimentally and serve as evidence in support of the K_{13} term or its disregard. In addition, the existence of the threshold for the anchoring energy is expected to be of some importance in the understanding of the temperature-induced surface transitions, where the anchoring orientation goes from planar to homeotropic (or vice versa). Equation (28) gives the temperature-dependent threshold for the anchoring energy W_p, since the curvature constants K, K_{24} and K_{13} depend on the nematic liquid crystal order parameter S. We note that the model of the surface transitions, based on the destabilizing effect due to the K_{13} term, was proposed in Ref. 24, where the authors have introduced a saturation elastic term to eliminate the discontinuity in the surface angles.

Our last remark concerns the one-constant approximation which is used throughout this paper for simplicity. There are no fundamental problems preventing a consideration of the elastic anisotropy to obtain more accurate quantitative results, but analytical treatment in this case, which leads to rather cumbersome expressions, can be shown not to change the effects qualitatively. We think it appropriate to refine the estimates on the basis of an experiment.

We gratefully acknowledge the financial support of the International Science Foundation under the Grant No. U58000.

[1] C. W. Oseen, Trans. Faraday Soc. **29**, 883 (1933).
[2] F. C. Frank, Discuss. Faraday Soc. **25**, 19 (1958).
[3] J. Nehring and A. Saupe, J. Chem. Phys. **54**, 337 (1971).
[4] V. M. Pergamenshchik, Ukrain. Fiz. Zhurnal **35**, 1352 (1990).
[5] G. Barbero, A. Sparavigna, and A. Strigazzi, Nuovo Cimento **12**, 1259 (1990).
[6] O. D. Lavrentovich and V. M. Pergamenshchik, Mol. Cryst. Liq. Cryst. **179**, 125 (1990).
[7] V. M. Pergamenshchik, Phys. Rev. E **47**, 1881 (1993).
[8] O. D. Lavrentovich, Phys. Scr. **39**, 349 (1991).
[9] G. P. Crawford, D. W. Allender, and J. W. Doane, Phys. Rev. A **45**, 8693 (1992).
[10] G. Barbero and C. Oldano, Mol. Cryst. Liq. Cryst. **170**, 99 (1989).
[11] H. P. Hinov, Mol. Cryst. Liq. Cryst. **148**, 197 (1987).
[12] V. M. Pergamenshchik, Phys. Rev. E **48**, 1254 (1993).
[13] G. Barbero and A. Strigazzi, Liq. Cryst. **5**, 693 (1989).
[14] S. Faetti, *The Abstracts of 15th Intern. Liq. Cryst. Conf.*, 407 (1994).
[15] A. Rapini and M. J. Papoular, J. de Physique **30**, C4-54 (1969).
[16] *Handbook of Mathematical Functions*, edited by M. Abramowitz and I. A. Stegun (National Bureau of Standards, 1964).
[17] S. Zumer and S. Kralj, Phys. Rev. A **45**, 2461 (1992).
[18] I. J. Ericksen, Phys. Fluids **9**, 1205 (1966).
[19] G. P. Crawford, D. W. Allender, and J. W. Doane, Phys. Rev. Lett. **67**, 1442 (1991).
[20] O. D. Lavrentovich and V. M. Pergamenshchik in *The Abstracts of 15th Intern. Liq. Cryst. Conf.*, 348 (1994).
[21] V. M. Pergamenshchik, P. I. J. Teixera, and T. J. Sluckin, Phys. Rev. E **48**, 1265 (1993).
[22] P. E. Cladis and M. Cleman, J. de Physique **33**, 591 (1972).
[23] A. D. Kiselev and V. Yu. Reshetnyak in Proc. SPIE, **1815**, 206 (1992).
[24] G. Barbero and G. Durand, Phys. Rev. E **48**, 1942 (1993).

Published in English in the original Russian journal. Edited by S. J. Amoretty